journal

J. Am. Ceram. Soc., **86** [7] 1176–81 (2003)

Evaluation of Mechanical Stability of a Commercial Sn88 Silicon Nitride at Intermediate Temperatures

Hua-Tay Lin,* Mattison K. Ferber,* and Timothy P. Kirkland*

Oak Ridge National Laboratory, Oak Ridge, Tennessee 37831-6068

Dynamic fatigue and stress rupture tests in four-point bending were conducted on a commercially available SN88 silicon nitride ceramic at temperatures in the range 700°–1000°C in air. The objective of the present study was to elucidate the failure of SN88 silicon nitride ceramic nozzles arising from a critical crack initiated at the intermediate temperature airfoil region during an engine field test. Results of dynamic fatigue tests indicated that SN88 silicon nitride tested at a stressing rate of 30 MPa/s exhibited little change in characteristic strength at the various test temperatures. However, SN88 silicon nitride exhibited a significant degradation in mechanical strength when tested at 0.003 MPa/s at temperatures indicative of a great susceptibility to slow crack growth, especially at 850°C. SEM and XRD analyses indicated that the mechanical instability of SN88 silicon nitride at intermediate temperatures resulted from the transformation of secondary phase(s) from oxidation. These phase transformations were accompanied by a large volume change, which led to the generation of large local residual tensile stresses. As a result, extensive damage zones were formed, which led to a substantial degradation of mechanical strength and reliability. Microstructural examination of failed SN88 airfoils indicated that a similar damage zone was formed in the regions exposed to intermediate temperatures during engine testing. Consequently, the ultimate failure of these vanes was attributed to the loss in mechanical strength from the damage zone formation.

I. Introduction

SILICON nitride ceramics with appropriate characteristics of the grain-boundary phase and with reinforcing elongated grain microstructure are leading candidates for use as high-temperature structural components in advanced gas turbines because of their superior thermomechanical properties.[1–5] Recent ceramic gas turbine programs, funded by the U.S. Department of Energy (DOE), at both Solar Turbines and Rolls Royce Allison[6–8] have conducted many field tests to increase the experience base concerning the behavior of ceramic components in industrial gas turbine environments. The Solar Turbines Program, for instance, was awarded the Ceramic Stationary Gas Turbine (CSGT) Development contract from the DOE in 1992.[9] The goals of this program were to improve turbine engine performance (fuel efficiency and output power) and reduce CO and NOx exhaust emissions. The approach involved retrofitting an existing gas turbine (4.14 MW; Model Centaur 50S) with silicon nitride nozzles, silicon nitride blades, and a SiC fiber-reinforced SiC ceramic matrix composite combustor liner.

In September 1998, a 100 h nozzle engine test was planned in which the engine would be subjected to cold and hot engine restarts and shutdown cycles that progressively increased in severity. The nozzles were fabricated from a commercially available SN88 silicon nitride ceramic (NGK Insulators, Ltd., Nagoya, Japan). The first engine test was successfully conducted, including one-hour full-load and 10 h total runtime. Subsequently, the second engine test was initiated for a 100 h endurance test. Note that the steady-state temperature during the engine test was estimated to be ~1120°C. However, the second test did not reach completion because borescope inspections, which were conducted after routine shutdown cycles, revealed severe cracking after 68 h of engine testing, including 15 start/stop cycles. The field test with SN88 silicon nitride nozzles was, therefore, terminated.

The selection of NGK SN88 silicon nitride for solar turbines' first-stage turbine nozzle application resulted from extensive mechanical testing and life-prediction modeling efforts.[10] The mechanical database generated for lifetime modeling covered the range of 1038°–1350°C in air. The test results indicated that SN88 exhibited excellent fatigue and creep performance at the temperature range used and no slow crack growth behavior at 1038°C in air. It was then expected that the SN88 silicon nitride would not be subject to any mechanical degradation induced by slow crack growth processes at temperatures <1000°C.

The cracking, which was observed on the airfoil surface of SN88 silicon nitride nozzles, initiated at the region near airfoil/platform transition region, as shown in Fig. 1(a). Finite-element-analysis of temperature distribution at steady-state (~1120°C) during engine operation indicated that the temperature in the airfoil/platform transition region ranged from 800°–900°C, as shown in Fig. 1(b).[11] Therefore, the failure of SN88 silicon nitride nozzles, which resulted from crack generation in the airfoil/platform transition region, would lead to the hypothesis that the SN88 silicon nitride might exhibit a mechanical instability at intermediate temperatures in an oxidizing environment. Recent studies conducted by Wereszczak *et al.* [12] have shown that some commercially available silicon nitride materials can exhibit substantial strength degradation at 850°C in air. The strength degradation observed was attributed to the change of state of secondary phases (i.e., softening of secondary phases), resulting in a significant increase in susceptibility to slow crack growth.

This paper describes the dynamic fatigue studies of a commercially available SN88 silicon nitride conducted over a temperature range of 700°–1000°C in air to evaluate its mechanical and microstructural stability. SEM analysis was used to correlate the changes in the microstructure and/or chemical compositions with the observed strength degradation. In addition, the stability of secondary phase(s) as a function of test temperature and loading rate was evaluated using XRD analysis.

II. Experimental Procedures

The SN88 silicon nitride material evaluated in the present study was gas-pressure-sintered using rare-earth sintering additives (NGK Insulators, Ltd., Nagoya, Japan). The predominant secondary crystalline phase present after densification is $Yb_4Si_2O_7N_2$, designated as the J-phase, as identified by XRD. Bend bar

M. Brito—contributing editor

Manuscript No. 186822. Received July 29, 2002; approved February 13, 2003.
*Member, American Ceramic Society.

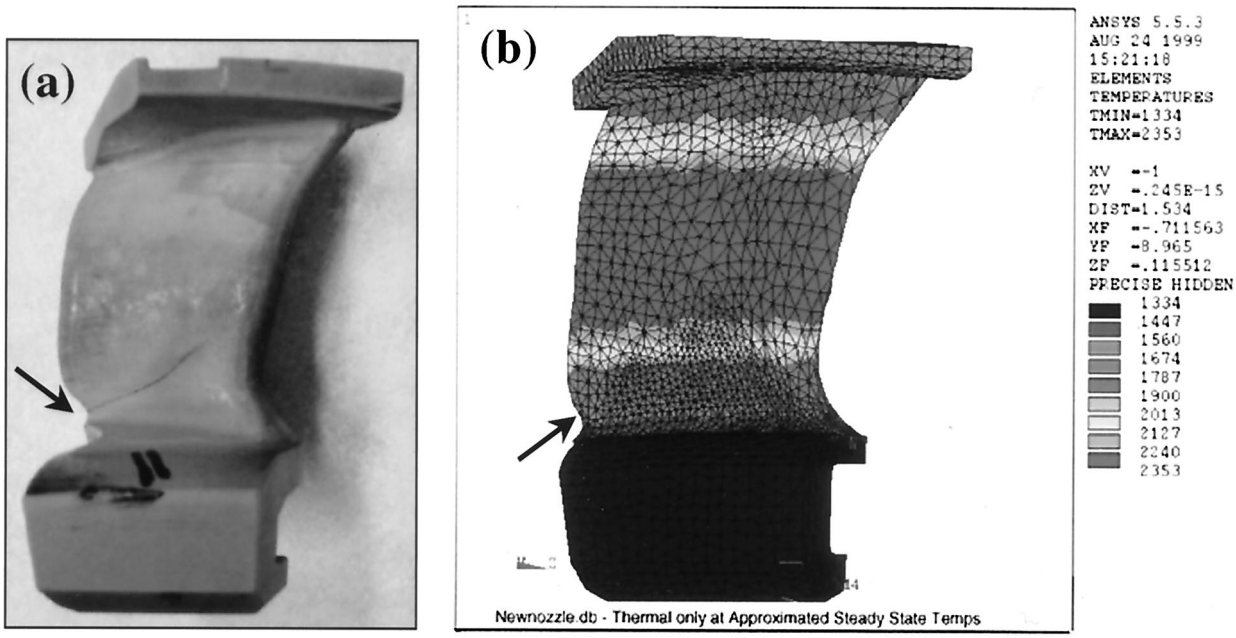

Fig. 1. (a) Macro photograph of SN88 silicon nitride nozzle after 68 h engine test with a critical crack developed at the airfoil/platform transition region. (b) FEA map showing temperature distribution in the silicon nitride nozzle at steady state (1120°C) during engine operation.

specimens with dimensions 3 mm × 4 mm × 50 mm were machined from purchased billets. Bend bars were longitudinally machined per ASTM C1161.[13] All specimens were also longitudinally chamfered.

Dynamic fatigue testing was conducted in four-point bending using 20/40 mm, α-SiC, semiarticulating fixtures at test conditions of 20°C and 30 MPa/s; 850°C and 30 MPa/s; and 850°C and 0.003 MPa/s in ambient air. The first two test conditions were chosen to compare the characteristic strength dependence on temperature, whereas the last two conditions were chosen to measure dynamic fatigue susceptibility at 850°C. To evaluate the temperature dependence of the dynamic fatigue susceptibility, tests were also conducted at 700°C and 1000°C and at 0.003 MPa/s. Each flexural testing system consisted of three load frames within a single furnace chamber. The pneumatic actuators were programmed to produce the desired loading (and corresponding stressing) rates via a personal computer through sintered α-SiC push rods. Load was continuously measured as a function of time, and flexure strength was calculated using ASTM C1161. On the failure of the last sample in the furnace chamber, the sensors interrupt the furnace power supply circuit to allow the bend bars to cool quickly to minimize damage and oxidation of the fracture surface of the last test bend bar.

Fractography and SEM analysis were performed on selected samples to provide insight into the dominant failure controlling process as a function of test temperature and stressing rate. XRS analysis was also conducted to compare the dominant secondary phase(s) present before and after dynamic fatigue tests at elevated temperatures in air. Polished cross sections for selected samples, which included fracture surface edges, were also prepared to elucidate the change in microstructure as a function of test conditions.

III. Results and Discussion

Figure 2 summarizes the dynamic fatigue response of SN88 silicon nitride tested at 850°C at stressing rates of 30 MPa/s and 0.003 MPa/s. Note that both SN282 and NT154 are used as a benchmark in this study. The SN282 (Kyocera Industrial Ceramics Corp., Vancouver, WA) contained ~7 wt% Lu_2O_3, whereas the NT154 (Saint-Gobain Ceramics & Plastics, Northboro, MA) contained ~4 wt% Y_2O_3 as sintering additive. Results showed that the fracture strength obtained for both SN282 and NT154 at 850°C was similar to that obtained at room temperature and was independent of stressing rates. Note that SN282 and NT154 exhibited a high fatigue exponent of 155 and 87, respectively, indicative of the absence of fatigue effects at this test temperature.

On the other hand, flexural strength of SN88 silicon nitride was very sensitive to stressing rates at 850°C. For instance, samples tested at 30 MPa/s exhibited a comparable strength to those obtained at room temperature (759 MPa versus 825 MPa), whereas samples tested at 0.003 MPa/s exhibited a substantial decrease in strength (~44%, from 825 MPa to 464 MPa). Consequently, SN88 silicon nitride exhibited a low fatigue exponent of 16, indicative of a high susceptibility to slow crack growth (SCG). The observed strength degradation at 850°C and 0.003 MPa/s was contradictory to the data reported previously,

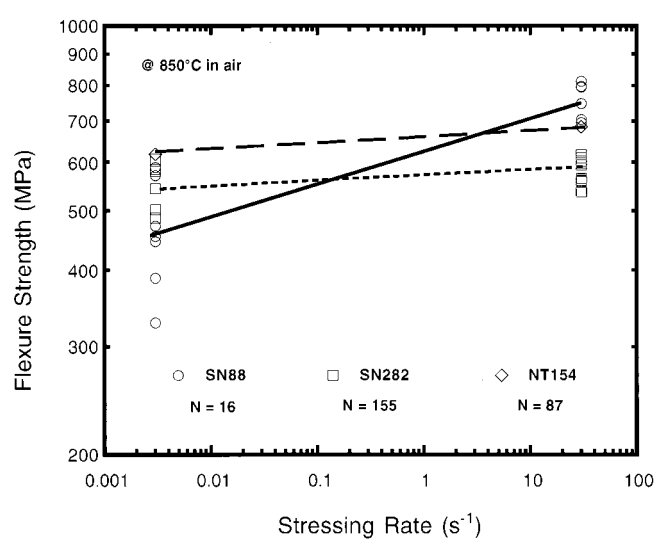

Fig. 2. Fracture strength of SN88 silicon nitride tested at 850°C at 30 MPa/s and 0.003 MPa/s in air. Results of SN282 and NT154 silicon nitride are used as a bench mark in the present study.

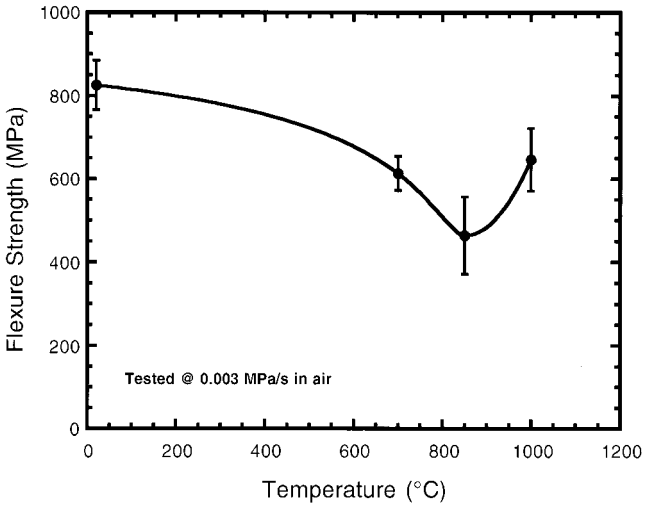

Fig. 3. Flexure strength of SN88 silicon nitride as a function of test temperature under 0.003 MPa/s stressing rate.

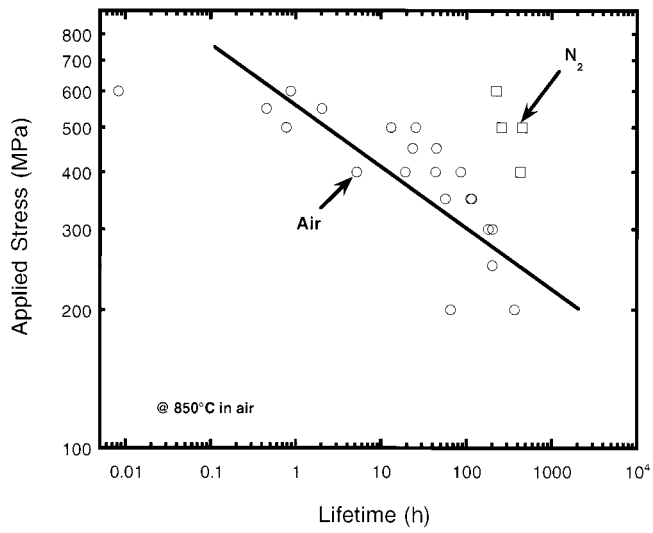

Fig. 4. Applied stress versus lifetime curve of SN88 silicon nitride tested at 850°C in air. Limited data were obtained in nitrogen environment.

which showed SN88 exhibiting excellent SCG and creep resistance at temperatures between 1038° and 1350°C.[10]

To understand how the test temperature influenced the extent of strength degradation, dynamic fatigue tests were also carried at 700° and 1000°C at 0.003 MPa/s. Figure 3 compares the flexural strength of SN88 as a function of test temperature at a stressing rate of 0.003 MPa/s. Results showed that the strength of SN88 decreased with an increase in test temperature with a minimum value occurring at 850°C and then increased with test temperature >850°C. Note that the strength obtained for SN88 at 700°C and 1000°C was comparable and ~24%–28% higher than that obtained at 850°C at the same stressing rate. Nonetheless, the strengths obtained at the low stressing rate at 700° and 1000°C were still 16%–19% lower than that obtained at 850°C and 30 MPa/s.

Because the SN88 exhibited a significant SCG susceptibility at 850°C, studies of stress rupture were subsequently conducted to understand how the applied stress levels influenced the lifetime of SN88 at 850°C. Figure 4 shows the lifetime versus applied stress data at 850°C. Results showed that the SN88 exhibited a strong stress-dependent lifetime behavior at stress levels as low as 200 MPa. For instance, the lifetimes of SN88 tested at 200 MPa ranged from 65 to 447 h. The SN88 also exhibited a low stress exponent of ~10, similar to the low fatigue exponent,[16] again indicative of a strong susceptibility to SCG at 850°C. Limited SN88 samples were tested in nitrogen to demonstrate that the observed mechanical degradation of SN88 was indeed related to oxidation-induced phenomenon. Nitrogen gas was continuously purged through the furnace chamber at a flow rate of 8 cm^3/s during the testing, and the measured oxygen content via an oxygen monitor (Centorr/Vacuum Industries, Nashua, NH) at the gas output line was <50 ppm. Results showed that the lifetime of SN88 obtained in nitrogen was at least two orders of magnitude longer than those obtained in air under the same applied stress level (Fig. 4).

Macroscopically, the fracture surface of SN88 samples tested at 0.003 MPa/s over the temperature range used or under stress rupture tests at 850°C revealed a light-colored layer on all surfaces of the bend bars (as shown in Fig. 5), indicating the presence of an environmentally affected zone (EAZ). The presence of the light-colored EAZ was similar to that observed in the crack region of the SN88 nozzle that failed after the 68 h engine test.[14] Note that the depth of the EAZ developed in SN88 samples after stress rupture tests increased with an increase in lifetime. SEM examinations of the fracture surfaces of SN88 tested at 0.003 MPa/s at 850°C indicated a change in the secondary phase microstructure, i.e., presence of pores,

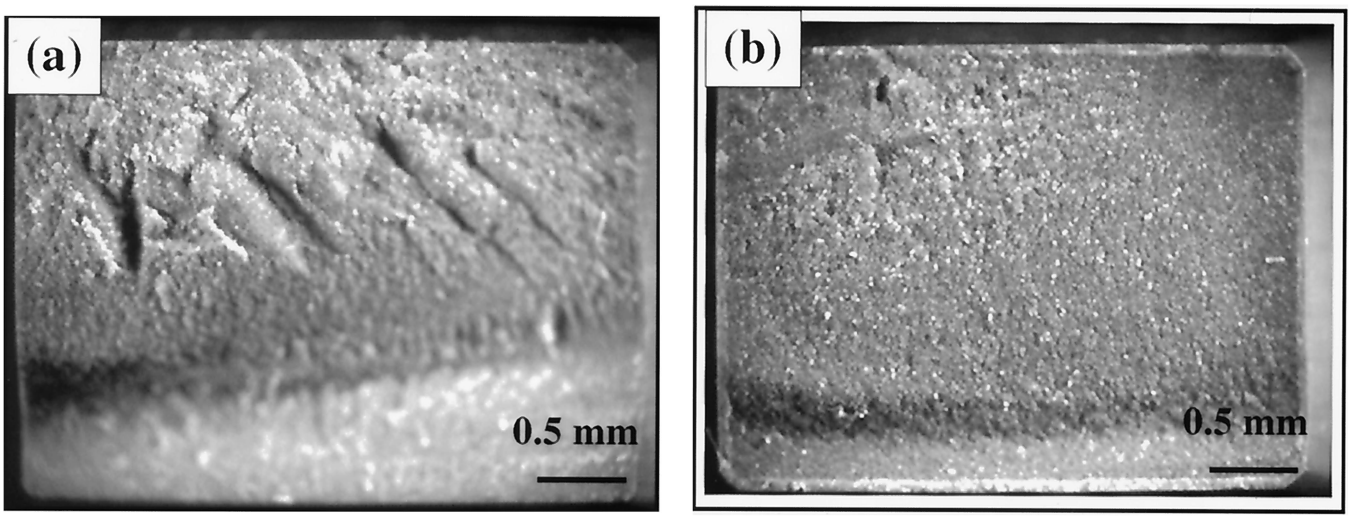

Fig. 5. Optical fractography of SN88 silicon nitride tested at 850°C at (a) 30 MPa/s and (b) 0.003 MPa/s. Note that the EAZ developed is ~125 μm.

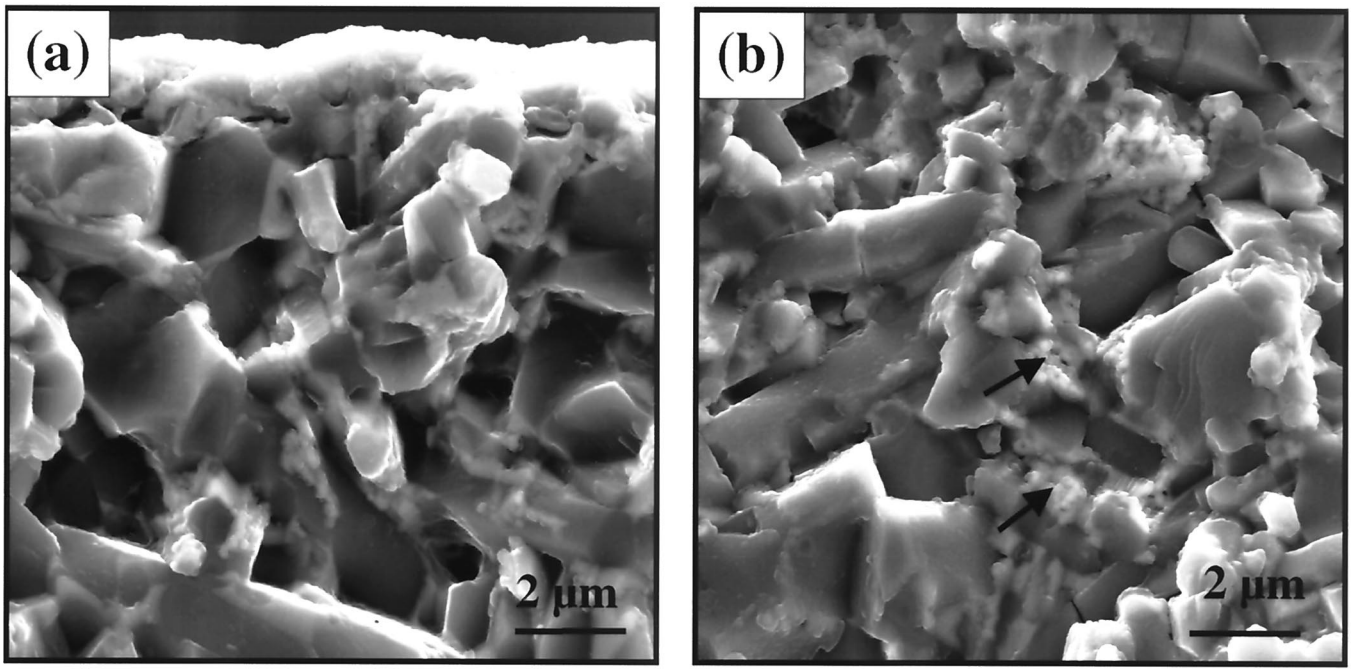

Fig. 6. SEM fracture surface of SN88 silicon nitride tested at 850°C at (a) 30 MPa/s and (b) 0.003 MPa/s. Arrows denote pores in secondary phase.

inside the EAZ. The change in secondary phase was not observed in material outside the EAZ or in the samples tested at the 30 MPa/s, as shown in Fig. 6. Similar features of an EAZ were also observed in all samples tested at 700° and 1000°C at 0.003 MPa/s and after stress-rupture tests at 850°C. Therefore, these SEM observations suggested that the EAZ developed in SN88 silicon nitride was a thermally activated, time-dependent process.

The EAZ became more prominent in polished cross sections of 0.003 MPa/s test samples. SEM observations revealed an ~30 μm damage zone, consisting of multiple cracks and pores in the secondary phase (Fig. 7(a)). The formation of an EAZ was observed in all four-sided surfaces, suggesting that the development of the EAZ was not a stress-promoted phenomenon, but solely oxidation-related. Figure 7(b) shows the development of a damaged microstructure in the compressive surface region. Results of XRD analysis for 0.003 MPa/s test samples indicated a change in the secondary phase from J-phase ($Yb_4Si_2O_7N_2$) to $Yb_2Si_2O_7$ plus Yb_2SiO_5, as shown in Fig. 8. Similar phase transformation of secondary phase was also observed in SN88 nozzles, which failed during the engine test.[14]

The phase transformation from J-phase to $Yb_2Si_2O_7$ plusYb_2SiO_5 could introduce a high residual tensile stress in the EAZ due to an ~71% decrease in material volume.[15,16] The material volume change can be estimated assuming the oxidation reaction is:

$$Yb_4Si_2O_7N_{2(s)} + SiO_{2(s)} + 3/2O_{2(g)} \rightarrow Yb_2Si_2O_{7(s)} + Yb_2SiO_{5(s)} + N_{2(g)} \quad (1)$$

Note that the molar volume of $Yb_4Si_2O_7N_2$ is 475.55 cm^3/mol, whereas the molar volume of $Yb_2Si_2O_7$ and Yb_2SiO_5 is 85.20 cm^3/mol and 62.40 cm^3/mol, respectively. Also, the molar volume of SiO_2 is 25.90 cm^3/mol. The development of a high tensile stress would then lead to the fracture of elongated Si_3N_4 grains and generation of intergranular cracks in the surface region of the bend bars. The formation of these through-surface flaws would result in a substantial decrease in mechanical strength and reliability. Similar mechanical instability at intermediate temperatures due to phase changes was previously reported for Si_3N_4 materials sintered with Y_2O_3 additive.[17–20]

For the case of oxidation-induced strength reduction, one can assume that the flaw size scales with the size of the oxidation affected zone that forms. This zone may be in the form of an oxide scale (typically silica) or a subsurface region into which the oxidant penetrates. In the present study, an oxidation induced damage zone extended from the surface into the bulk, as shown in Fig. 7. Figure 9 illustrates the size of this damage zone as measured by SEM as a function of time to failure. The rate of growth, which was linear with time, was estimated from a regression analysis as 0.58 μm/h. For a constant stress test, the strength degrades with time in accordance with the expression

$$S_f = \frac{K_{IC}}{Y(a_o + 0.58t)^{\frac{1}{2}}} \quad (2)$$

where Y is geometry factor, a_o is the initial crack size, and t is the time in hours.[21] Failure occurs when the strength becomes equal to the applied stress. Taking Y as $\sqrt{\pi}$, a_o as 20 μm, and K_{1C} as 5.5 MPa $m^{1/2}$ as typical values for the SN88 silicon nitride, one can generate a stress rupture curve (Fig. 10). The experimental data in this figure agree quite well with the predictions. For the case of dynamic fatigue, failure will occur when the applied stress, which increases linearly with time, exceeds the strength as defined by Eq. (2). Figure 11 compares the predicted strength and experimental data as a function of stressing rates. Once again, the agreement is reasonably good.

Results of dynamic fatigue and stress rupture tests at 850°C in air suggested that an EAZ developed in the airfoil/platform transition region of SN88 silicon nozzles, where the temperature was low and no protective silica layer would form during the exposure. The generation of extensive multiple cracks in the EAZ would significantly reduce the mechanical reliability and, thus, greatly increase the susceptibility of nozzles to SCG processes during engine testing. Consequently, a critical crack could readily initiate at the airfoil/platform transition region and lead to the failure of the nozzles. On the other hand, the reason that the EAZ was not observed in the higher temperature regions, i.e., middle airfoil region, appeared to be due to rapid formation of a silica scale, which prevented the ingress of the oxidant into the bulk. Based on other studies of airfoils, the material subjected to the higher temperatures would be expected to exhibit significant recession due to the competing effects of silica scale volatilization and oxidation.

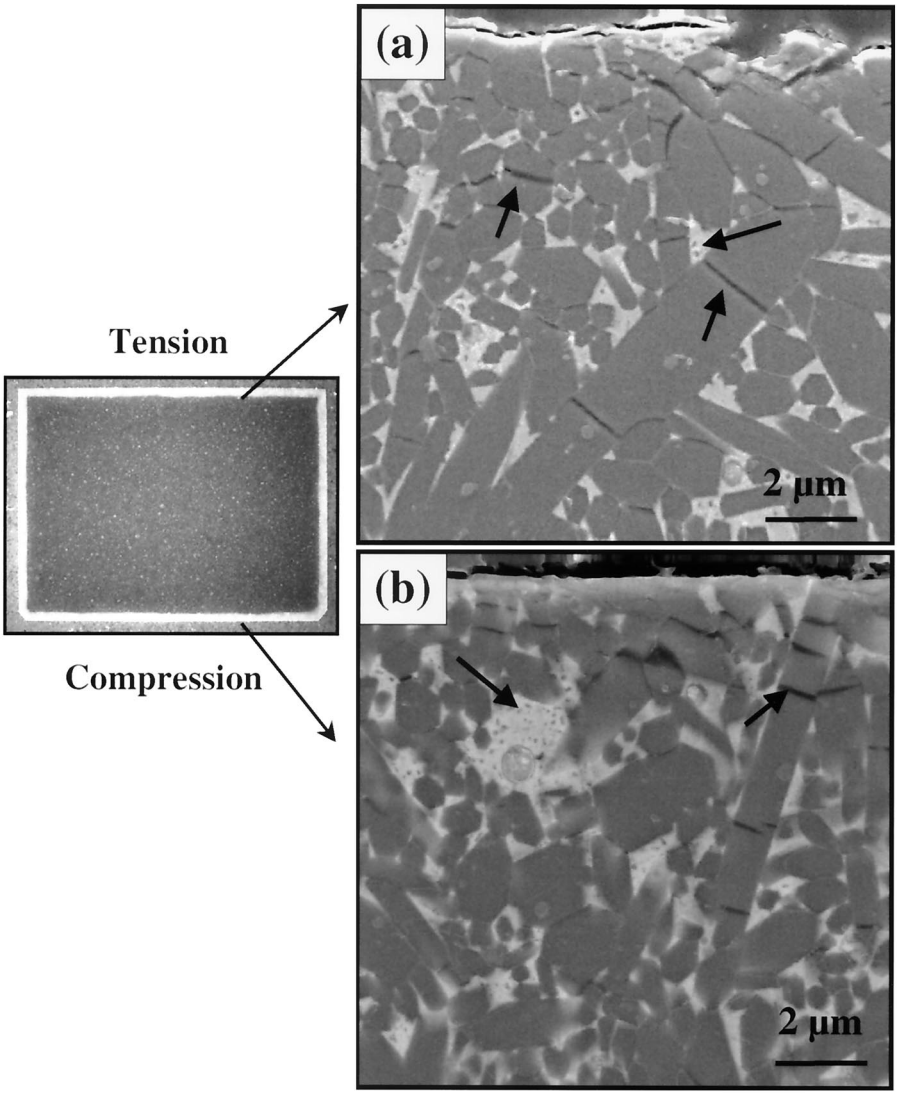

Fig. 7. SEM micrographs of polished cross section of SN88 silicon nitride tested at 850°C at 0.003 MPa/s taken from (a) tensile surface region and (b) compressive surface region. Arrows denote pores in secondary phase and fracture of silicon nitride grains and grain boundaries.

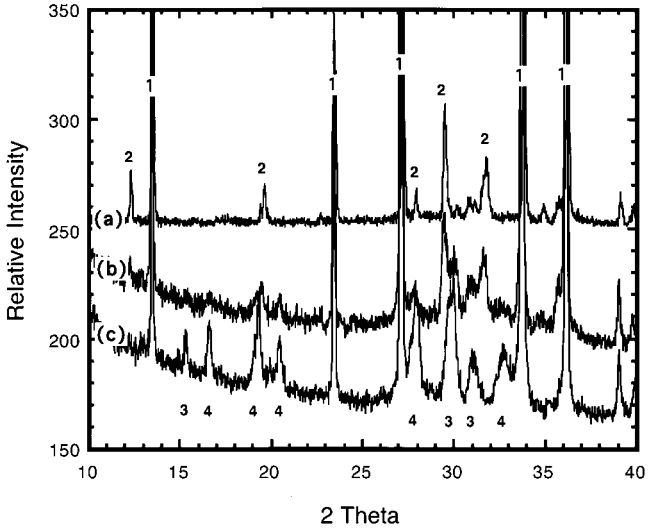

Fig. 8. X-ray spectra of SN88 silicon nitride in as-received (a), after tested at 850°C, 30 MPa/s (b), and after tested at 850C, 0.003 MPa/s (c). 1 denotes β-Si_3N_4, 2 denotes J-phase ($Yb_4Si_2O_7N_2$), 3 denotes Yb_2SiO_5, and 4 denotes $Yb_2Si_2O_7$, respectively.

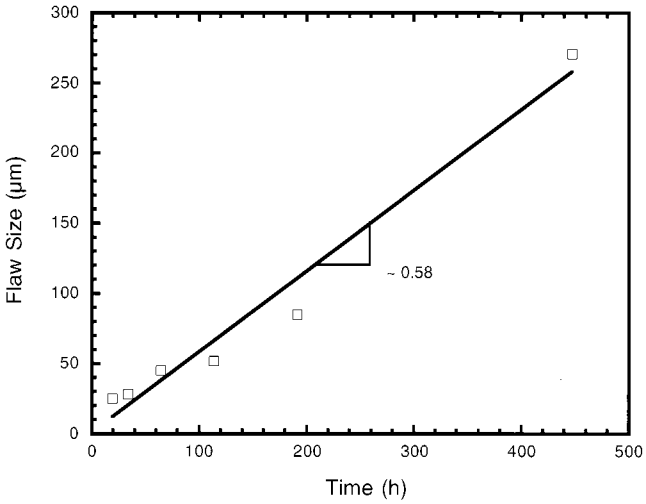

Fig. 9. Flaw size (damage zone) developed as a function of specimen lifetime.

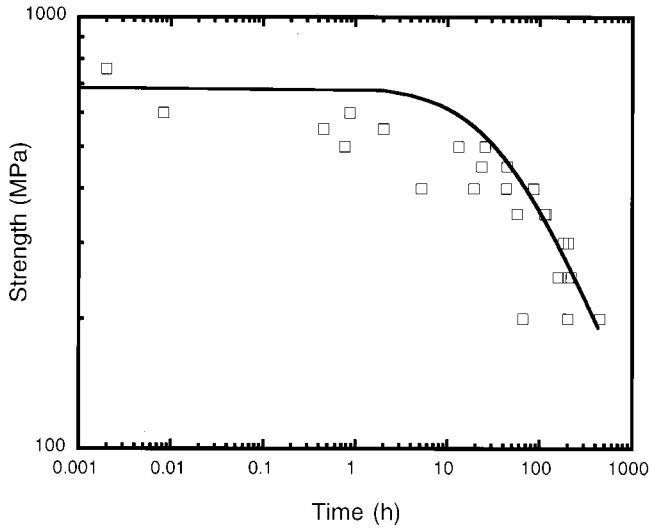

Fig. 10. Predicted strength versus time curve for SN88 silicon nitride. Note that the lifetime-stress data agree well with the prediction.

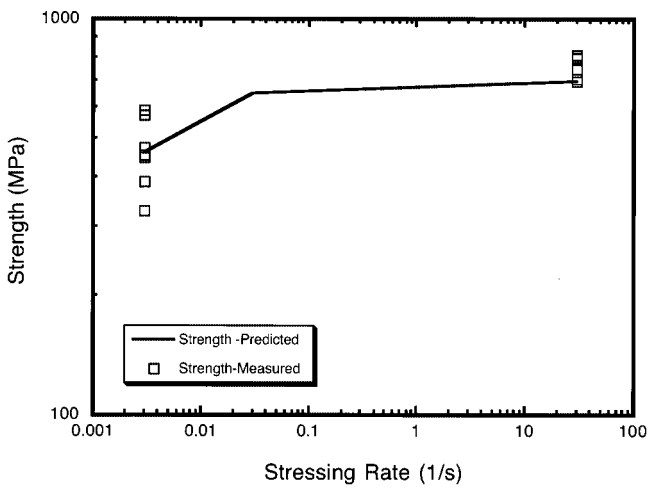

Fig. 11. Predicted flexure strength of SN88 silicon nitride as a function of stressing rates. Note that the measured strength agrees well with the prediction.

IV. Summary

Studies of dynamic fatigue and stress rupture at intermediate temperatures in air were conducted on SN88 silicon nitride to elucidate the failure mechanism of SN88 silicon nitride nozzles during field test in an industrial gas turbine. Mechanical results showed that the SN88 silicon nitride exhibited a significant strength reduction accompanied by a low fatigue exponent when tested at 850°C in air, indicative of a great susceptibility to SCG. The subsequent stress rupture tests showed that SN88 exhibited a strong dependence of lifetime on applied stress level and further confirmed the mechanical instability at 850°C in air. Both SEM and XRD analyses indicated mechanical instability of SN88 silicon nitride at intermediate temperatures in air resulted from the phase transformation of secondary phase(s) from oxidation. The phase transformation, accompanied by a large material volume change, would lead to the generation of a large residual tensile stress. Subsequently, an extensive microstructural damage zone would form in the surface region, resulting in substantial degradation of mechanical strength and reliability. The substantial decrease in mechanical strength and reliability of SN88 silicon nitride at intermediate temperatures in an oxidizing environment would ultimately lead to the failure of turbine nozzles.

Acknowledgments

The authors thank Drs. S. D. Nunn, J. O. Kiggans Jr., and P. F. Becher for reviewing the manuscript and their helpful discussions. Research is sponsored by the U.S. Department of Energy, Office of Power Technologies, Microturbine Materials Program, under Contract DE-AC05–00OR22725 with UT-Battelle, LLC.

References

[1]D. Anson, K. S. Remesh, M. DeCorso, "Application of Ceramics in Industrial Gas Turbines; Taks 1, Technology Background," Taks 1 Report, DOE/CE/40878–1&2; Battelle, Columbus, March 1991.

[2]D. Anson, W. J. Sheppard, and W. P. Parks Jr., "Impact of Ceramic Components in Gas Turbines for Industrial Generation," *Am. Soc. Mech. Eng.* Paper No. 92-GT-393, 1992.

[3]H. E. Helms, R. A. Johnson, and L. E. Groseclose, "AGT 100-Advanced Gas Turbine Technology Development Project"; pp. 137–55 in *Proceedings of the 23rd Automotive Technology Development Contractors' Coordination Meeting P-165* (Warrendale, PA, March, 1986). U.S. Department of Energy, Washington, DC.

[4]M. van Roode, "Ceramic Retrofit Program," *Proceedings of the Joint Contractors Meeting: FE/EE Advanced Turbine Systems Conference FE Fuel Cells and Coal-Fired Heat Engines Conference*, DOE/METC-93/6132, 77–93, 1993.

[5]D. Carruthers and L. Lindberg, "Critical Issues for Ceramics for Gas Turbines"; pp. 1258–72 in *Proceedings of the 3rd International Symposium on Ceramic Components and Materials for Engines*, American Ceramic Society, Westerville, OH, 1988.

[6]V. Parthasarathy, M. van Roode, J. Price, S. Gates, S. Waslo, and P. Hoffman, "Review of Solar's Ceramic Stationary Gas Turbine Development Program," *Proceedings of 6th International Symposium on Ceramic Materials and Components for Engines*, Arita, Japan, 259–64, Technoplaza Co., Ltd., Tokyo, Japan, 1997.

[7]R. Wenglarz, S. Calcuttawala, and J. E. Pope, "Ceramics Vane Demonstration in an Industrial Turbine," *Am. Soc. Mech. Eng.* Paper No. 97-GT-155, 1997.

[8]P. Khandelwal and P. Heitman, "Ceramic Gas Turbine Development at Rolls-Royce in Indianapolis"; pp. 111–132, in *Ceramic Gas Turbine Design and Test Experience*. Edited by M. van Roode, M. K. Ferber, and D. W. Richerson. American Society of Mechanical Engineers, New York, 2002.

[9]W. D. Brentnall, M. van Roode, P. F. Norton, S. Gates, J. R. Price, O. Jimenez, and N. Miriyala, "Ceramic Gas Turbine Development at Solar Turbines Incorporated"; pp. 155–92, in *Ceramic Gas Turbine Design and Test Experience*. Edited by M. van Roode, M. K. Ferber, and D. W. Richerson. American Society of Mechanical Engineers, New York, 2002.

[10]A. A. Wereszczak and T. P. Kirkland, "Creep Performance of Candidate SiC and Si_3N_4 Materials for Land-Based, Gas Turbine Engine Components," *Am. Soc. Mech. Eng.* Pap. No. 96-GT-385, 1996.

[11]M. van Roode at Solar Turbines, San Diego, California; personal communication.

[12]A. A. Weresczak, T. P. Kirkland, H. T. Lin, and S. K. Lee, "Intermediate Temperature Inert Strength and Dynamic Fatigue of Candidate Silicon Nitrides for Diesel Exhaust Valves," *Ceram. Eng. Sci. Proc.*, **21** [4] 497–508 (2000).

[13]"Standard Test Method for Flexural Strength of Advanced Ceramics at Ambient Temperatures," ASTM Designation C1161, *1999 Book of ASTM Standards*, Vol. 15.01. American Society for Testing and Materials, West Conshohocken, PA.

[14]H. T. Lin, M. K. Ferber, and M. van Roode, "Mechanical Reliability of Si_3N_4 Nozzles After Exposure in an Industrial Gas Turbine"; pp. 97–102 in *Proceedings of the 7th International Symposium on Ceramic Materials and Components for Engines*. Edited by J. G. Heinrich and F. Aldinger. Wiley-Vch, New York, 2001.

[15]R. R. Wills, R. W. Stewart, J. A. Cunningham, and J. M. Wimmer, "The Silicon Lanthanide Oxynitrides," *J. Mater. Sci.*, **11**, 749–59 (1976).

[16]Powder Diffraction File, PDF Card No. 37–0458 ($Yb_2Si_2O_7$) and #40–0386 (Yb_2SiO_5). International Centre for Diffraction Data, Newtown Square, PA, 2002.

[17]F. F. Lang, S. C. Singhal, and R. C. Kuznicki, "Phase Relationship and Stability Studies in the Si_3N_4–SiO_2–Y_2O_3 Pseudoternary System," *J. Am. Ceram. Soc.* **60**, [5–6] 249–52 (1997).

[18]F. F. Lange, "High Temperature Deformation and Fracture Phenomena of Polyphase Si_3N_4 Materials," *Proceedings of the 2nd NATO Advanced Study Institute of Nitrogen Ceramics* 467, Martinus Nijhoff Publishers, The Hague, Netherlands, 1981.

[19]C. L. Quackenbush and J. T. Smith, "Phase Effects on Si_3N_4 Containing Y_2O_3 or CeO_2: II, Oxidation," *J. Am. Ceram. Soc.* **59** [5] 533–37 (1980).

[20]R. T. Govila, "Fracture and Intermediate Temperature Instability in Yttria-Doped Hot-Pressed Silicon Nitrides," *Am. Ceram. Soc. Bull.*, **65**, 1287–92 (1986).

[21]S. M. Wiederhorn, "Subcritical Crack Growth in Ceramics"; pp. 613–46 in Fracture Mechanics of Ceramics Vol. 2: *Microstructure, Materials, and Applications*. Edited by R. C. Bradt, D. P. H. Hasselman, and F. F. Lange, Plenum Press, New York, 1974. □